Imaging of tumor hypoxia with [124I]IAZA in comparison with [18F]FMISO and [18F]FAZA – first small animal PET results

Gerald Reischl [1], Donna S. Dorow [2,3], Carleen Cullinane [2], Andrew Katsifis [4], Peter Roselt [3], David Binns [3], Rodney J. Hicks [2,3]

[1] Radiopharmacy, PET-Center, University of Tübingen, Tübingen, Germany; [2] Translational Research Laboratory, Trescowthick Research Laboratories, Peter MacCallum Cancer Institute, Melbourne, Victoria, Australia; [3] Centre for Molecular Imaging, Peter MacCallum Cancer Institute, Melbourne, Victoria, Australia; [4] Radiopharmaceuticals Research Institute, Australian Nuclear Science and Technology Organisation, Sydney, NSW, Australia

ABSTRACT – **Purpose:** This study was performed to compare the 2-nitroimidazole derivatives [124I]IAZA, [18F]FAZA and well known [18F]FMISO in visualization of tumor hypoxia in a mouse model of human cancer using small animal PET. **Methods:** PET imaging of female Balb/c nude mice bearing A431 tumors on a Phillips Mosaic small animal PET scanner was performed 3 h p.i. for all three tracers. Mice injected with [124I]IAZA were scanned again after 24 h and 48 h. In addition to the mice breathing air, in the case of [18F]FAZA and [124I]IAZA a second group of mice for each tracer was kept in an atmosphere of carbogen gas (5 % of CO_2 + 95 % of O_2; from 1 h before to 3 h after injection) to evaluate the oxygenation dependency on uptake (all experiments n = 4). After the final PET scan animals were sacrificed and biodistribution was studied. **Results:** Mice injected with [18F]FAZA displayed significantly higher tumor-to-background (T/B) ratios (5.19 ± 0.73) compared to those injected with [18F]FMISO (3.98 ± 0.66; P < 0.05) or [124I]IAZA (2.06 ± 0.26; P < 0.001) 3 h p.i. Carbogen breathing mice showed lower ratios ([18F]FAZA: 4.06 ± 0.59; [124I]IAZA: 2.02 ± 0.36). The T/B ratios increased for [124I]IAZA with time (24 h: 3.83 ± 0.61; 48 h: 4.20 ± 0.80), but after these late time points the absolute whole body activity was very low, as could be seen from the biodistribution data (< 0.1 %ID/g for each investigated organ) and ratios were still lower than for [18F]FAZA 3 h p.i. Due to de-iodination uptake in thyroid was high. Biodistribution data were in good agreement with the PET results. **Conclusions:** [18F]FAZA showed superior biokinetics compared to [18F]FMISO and [124I]IAZA in this study. Imaging at later time points that are not possible with the short-lived 18F-labeled tracers resulted in no advantage for [124I]IAZA, i. e., tumor-to-normal tissue ratios could not be improved.

INTRODUCTION

Oxygen deficiency is a common characteristic of solid tumors leading to decreased sensitivity to radiation therapy and anticancer drugs. Therefore, hypoxia is an important adverse prognostic factor for tumor progression and resistance to therapy (1-3) and identification of hypoxic tumor tissue is of high clinical relevance.

Positron emission tomography (PET) offers the possibility to detect hypoxia non-invasively in vivo (4). To date the most commonly used tracer to visualize and quantify hypoxia using PET has been [18F]fluoromisonidazole ([18F]FMISO; Figure 1) (5-8). Its uptake mechanism has been validated to be oxygenation-specific (9,10). More recently, the 18F labeled azomycin arabinoside ([18F]FAZA; Figure 1; ref. 11) has been investigated and found to have superior pharmacokinetics compared to [18F]FMISO. This is primarily due to faster clearance from normal tissue resulting in an enhanced tumor-to-background ratio (12-14). Another azomycin-based nucleoside iodoazomycin arabinoside (IAZA; Figure 1) has been labeled with various iodine isotopes (^{123}I, ^{125}I and ^{131}I) and proved its value for detection of hypoxia in vitro (15) and in vivo (16,17). PET imaging using IAZA labeled with iodine-124 ($T_{1/2}$: 4.18 d; $I_{\beta+}$: 25 %) has not been reported to date. However, [124I]iodo-azomycin galactoside was studied in small animal PET experiments in tumor bearing mice and demonstrated its potential for hypoxia imaging (18).

Corresponding Author: Dr. Gerald Reischl Radiopharmacy, PET-Center University of Tübingen Röntgenweg 15 D-72076 Tübingen Germany Email: gerald.reischl@uni-tuebingen.de
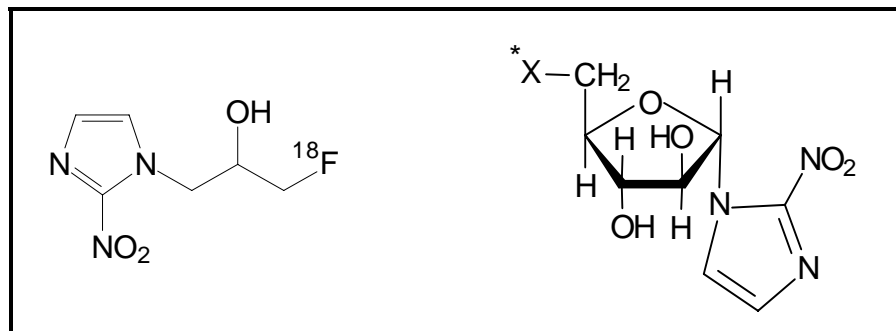
Figure 1: Chemical structures of [18F]FMISO (left) and the azomycin (i.e. 2-nitroimidazole) arabinoside derivatives (right) for [18F]FAZA (*X = 18F) and [124I]IAZA (*X = 124I).

Recent adaptation of PET for use with small animals has created a valuable opportunity for in vivo characterization of molecular mechanisms regulating tumor phenotype such as hypoxia.

Herein we report results of a comparative small animal imaging study, for the first time comparing [124I]IAZA, [18F]FAZA and [18F]FMISO PET together with biodistribution studies. Iodine-124 offers the opportunity of imaging at late time points (here 24 h and 48 h) to investigate possible enhancement of hypoxia imaging, compared to imaging at 3 h p. i. with [18F]FAZA or the more widely used hypoxia tracer [18F]FMISO. To demonstrate the oxygen dependence of tracer uptake, animals were divided into groups, breathing either air or carbogen.

METHODS

Materials

[18F]Fluoromisonidazole ([18F]FMISO) was purchased from the Austin Hospital PET Centre, Melbourne. Specified radiochemical purity was > 95 % and specific activity was between 55 and 111 GBq/µmol at end of synthesis (EOS). Sodium [124I]iodide was from Ritverc, St. Petersburg, Russia. [18F]Fluoride was produced in house (Peter MacCallum Cancer Institute) using an OSCAR 7 cyclotron (Oxford Instruments, Oxford, UK) by the $^{18}O(p,n)^{18}F$ nuclear reaction. The precursor for [18F]FAZA and [124I]IAZA synthesis was a kind gift from Drs. Leonard I. Wiebe and Piyush Kumar, University of Alberta, Canada. [18F]FAZA was labeled as described previously (19,20), using a TRACERlab MX synthesizer (GE Healthcare, Liège, Belgium)

coupled with a preparative HPLC system. The product was obtained in a radiochemical purity of > 98 % and a specific activity of 118 GBq/µmol (EOS). [124I]IAZA was prepared by isotopic [124I]iodine exchange using modified literature methods (21) yielding the product in > 97 % radiochemical purity. Specific activity was 41 GBq/µmol (EOS). Final purity, radiochemical identity and specific activity of tracers were assessed by HPLC, following standard protocols.

Tumor growth, implantation and imaging

All experiments complied with current laws of Australia including ethics approval. A431 human squamous cell carcinoma cells (ATCC) were cultured in alpha MEM supplemented with 10 % FBS in 5 % CO_2 in air at 37°C. Female Balb/c nude mice 8-11 weeks old were inoculated s.c. on the right forelimb with 3×10^6 A431 cells in PBS. Tumors were measured twice weekly using electronic calipers and tumor volumes calculated using the formula [volume = length/2 x width^2]. Once tumor volumes had reached an average of 150 mm^3, animals were randomized into 5 groups of 4 animals per group. Animals were injected via lateral tail vein with 14-22 MBq [18F]FMISO, [18F]FAZA or [124I]IAZA in 100 µL of saline. Four animals to be injected with [18F]FAZA and [124I]IAZA were kept in a chamber equilibrated with carbogen gas (5% CO_2 in O_2) for one hour prior to injection and during the first 3 h tracer uptake period while the remaining mice were kept in room air during this period. There was no disturbance to their food and water supply.

Animals were anaesthetized by inhalation of 2.5 % isoflurane / 50 % O_2 in air (flow rate 200 mL/min) approximately 3 h post-tracer injection

and scanned for 5 – 10 min on a Phillips Mosaic small animal PET scanner. Animals injected with [124]IAZA were rescanned at 24 and 48 h post injection. PET images were reconstructed using the OSEM algorithm (22,23) and images displayed using standard image software available on the scanner. Tracer uptake was measured using region-of-interest (ROI) software on the scanner workstation. Briefly, elliptical ROIs were manually placed around the tumor and a background region on transaxial slice images displayed on the workstation. The background ROI was chosen to represent tracer present within the blood pool and non-tumor tissue, excluding regions of increased uptake such as GI tract. Maximum, minimum and average pixels within the ROI per slice were automatically stored as data files. Uptake ratios were calculated by dividing the maximum value of pixels within a tumor ROI by the average value of pixels within the background ROI. The resolution of the Mosaic scanner is 2.2 mm and the average tumor diameter for all groups of animals was greater than 4 mm on all imaging days, therefore correction for partial volume effect was not required. The axial FOV of the scanner is 12 cm, which encompassed the whole of the mouse during scanning.

Biodistribution
Following final PET scans animals were sacrificed. Blood, tumor and a range of tissues were removed, washed with saline if necessary, then weighed and placed into flat bottom tubes. Disintegrations at 511 keV ± 15 % were quantified in a well counter (187-950-A100 MCA, Biomedex Medical Systems) attached to a multichannel analyzer interfaced with Atomlabs 950 software (Biomedex Medical Systems).

Statistics
Results are expressed as mean values of parameters ± standard deviation (SD). Unpaired student's t tests were used to determine the statistical significance of differences between measured quantities in groups of animals. $P < 0.05$ was considered statistically significant.

RESULTS

Biodistribution data
Data for tissue uptake of [18F]FMISO and [18F]FAZA 3 h post injection and of [124]IAZA after 48 h are presented in Table 1. For all organs uptake was substantially higher for [18F]FMISO than for [18F]FAZA with the largest differences for lung, liver, kidneys and small intestine (more than a factor of 3). The organ with the highest uptake was the liver for both markers. Clearance from blood was much faster for [18F]FAZA. Tumoral uptake of [18F]FMISO (3.43 ± 0.77) was approximately two times higher than for [18F]FAZA (1.88 ± 0.17). Nevertheless, tumor-to-blood ratio was significantly higher for [18F]FAZA (5.13 ± 0.75 compared to 3.33 ± 0.20 for [18F]FMISO; $P < 0.01$), while for tumor-to-muscle ratios this effect was less marked (3.05 ± 0.73 vs. 2.76 ± 0.73). Comparison of [18F]FAZA uptake in mice breathing air or carbogen showed lower tumor-to-blood and tumor-to-muscle ratios for the latter, as expected (T/Bl: 5.13 ± 0.75 vs. 3.99 ± 0.54; T/M: 3.05 ± 0.73 vs. 1.99 ± 0.90). Interestingly, tumor uptake showed no significant difference, but background uptake in non-tumor tissues was higher in the case of carbogen breathing animals.

In the case of [124]IAZA animals were sacrificed directly after the 48 h PET scan and tissue uptake values determined. After 48 h of uptake the overall radioactivity in all tissues was below 0.1 %ID/g, even in tumors. Tumor-to-muscle ratios were significantly higher than for [18F]FAZA after 3h of uptake, both for air ($P < 0.002$) and for carbogen ($P < 0.001$) breathing mice. The difference in tumor-to-blood or tumor-to-muscle ratios was lower for [124]IAZA comparing air and carbogen breathing animals (T/Bl: 5.28 ± 0.29 vs. 5.02 ± 0.44; T/M: 6.59 ± 1.05 vs. 5.74 ± 0.31), possibly due to an equalizing effect within 48 h, as carbogen breathing was stopped after 3 h.

Animal PET imaging
In all PET images, uptake was clearly visible in tumors for all three tracers, i.e. for [18F]FMISO and [18F]FAZA 3 h p.i. and [124]IAZA after 3 h, 24 h and 48 h. Comparison of the quantitative analysis of the tumor-to-background ratios from imaging data after 3 h is presented in Figure 2 in mice breathing air, T/B ratio was significantly higher for [18F]FAZA than for [18F]FMISO (5.19 ± 0.73 vs. 3.98 ± 0.66; $P < 0.05$). At this time point T/B ratio for [124]IAZA was much lower and there was no difference between animals

Table 1: Effect of carbogen breathing on biodistribution of PET hypoxia tracers in tissues of A431 tumor bearing mice.

Tissue	[^{18}F]FMISO[a] Air	[^{18}F]FAZA[b] Air	Carbogen	[^{124}I]IAZA[c] Air	Carbogen
Blood	1.034 ± 0.225	0.375 ± 0.075	0.449 ± 0.071	0.016 ± 0.002	0.020 ± 0.002
Heart	0.732 ± 0.331	0.482 ± 0.070	0.618 ± 0.089	0.026 ± 0.006	0.032 ± 0.004
Lung	1.236 ± 0.438	0.339 ± 0.052	0.477 ± 0.075	0.018 ± 0.001	0.023 ± 0.003
Liver	4.548 ± 2.100	1.325 ± 0.384	2.401 ± 1.285	0.057 ± 0.003	0.075 ± 0.011
Spleen	0.877 ± 0.307	0.347 ± 0.033	0.528 ± 0.124	0.011 ± 0.001	0.012 ± 0.001
Kidney	1.621 ± 0.640	0.488 ± 0.099	0.798 ± 0.290	0.025 ± 0.002	0.030 ± 0.003
Muscle	1.259 ± 0.167	0.655 ± 0.211	1.079 ± 0.590	0.013 ± 0.002	0.017 ± 0.002
Stomach	0.865 ± 0.253*	0.550 ± 0.058	0.634 ± 0.323	0.040 ± 0.011	0.039 ± 0.003
Small intestine	2.196 ± 1.112	0.629 ± 0.051	0.965 ± 0.388	0.010 ± 0.001	0.011 ± 0.002
Tumor	3.433 ± 0.770	1.883 ± 0.170	1.794 ± 0.418	0.086 ± 0.005	0.097 ± 0.013
T/Bl ratio	3.325 ± 0.201	5.132 ± 0.750	3.988 ± 0.537	5.284 ± 0.289	5.016 ± 0.443
T/M ratio	2.764 ± 0.725	3.050 ± 0.734	1.988 ± 0.904	6.590 ± 1.053	5.740 ± 0.306

a) Radioactivity in tissues of animals breathing room air at 3h after injection of [^{18}F]FMISO.
b) Animals breathing either air or carbogen at 3h after injection of [^{18}F]FAZA.
c) Animals breathing either air or carbogen at 48 h after injection of [^{124}I]IAZA.
Note: Data are presented as %ID/g ± SD; n = 4, *n = 3.

breathing air (2.06 ± 0.26) and carbogen (2.02 ± 0.36). In case of [^{18}F]FAZA, mean T/B ratio was approximately 20 % lower in mice breathing carbogen (4.06 ± 0.59).

In mice injected with [^{124}I]IAZA tumor-to-background activity contrast increased much more slowly than that for [^{18}F]FMISO and [^{18}F]FAZA. Figure 3 shows representative images of 2 air breathing mice at 3 h, 24 h and 48 h post [^{124}I]IAZA injection. As can be seen, T/B ratio increased with time; at 3 h p.i. most of the radioactivity was in the abdomen and the intestinal tract. The 24 h p.i. scans showed little background activity, excepting stomach and thyroid, as animals did not receive thyroid blockade with iodine supplementation. This most likely reflects substantial de-iodination of IAZA in vivo. Images at 48 h looked similar to those at 24 h, however, the total activity remaining was quite low.

The quantitative data (Figure 4) show an increase in T/B ratio at 24 h in mice breathing air to 3.83 ± 0.61 and to 4.20 ± 0.80 at 48 h. In mice breathing carbogen the ratio was 3.47 ± 0.52 at 24 h and 3.44 ± 0.88 at 48 h p.i. Although the tumor-to-background ratios increased for mice injected with [^{124}I]IAZA with time, they were still lower than for those injected with [^{18}F]FAZA after 3 h (4.20 ± 0.80 and 3.44 ± 0.88 vs. 5.19 ± 0.73 and 4.06 ± 0.59). The difference in T/B ratio between mice breathing air and mice breathing carbogen was less marked for [^{124}I]IAZA than for [^{18}F]FAZA, although there appears to be a trend toward reduced T/B ratio in the [^{124}I]IAZA carbogen group over time (Figure 4).

DISCUSSION

Tumor hypoxia can lead to a reduced sensitivity to radiation and anticancer drugs. As tumor hypoxia seems to be a predictive factor for tumor response to therapy, its measurement may be
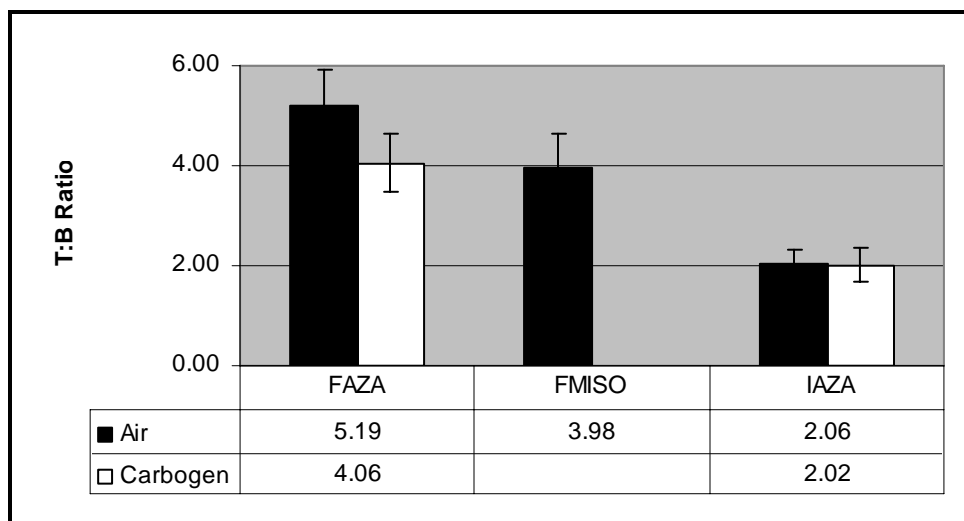
Figure 2: Tumor uptake of PET tracers based on image analysis. Tumor-to-background ratios 3 h p.i. of [^{18}F]FMISO, [^{18}F]FAZA and [^{124}I]IAZA in Balb/c nude mice bearing A431 tumor, breathing either air or carbogen (Data are presented as mean with error bars indicating SD; for SD numbers see text; n = 4).
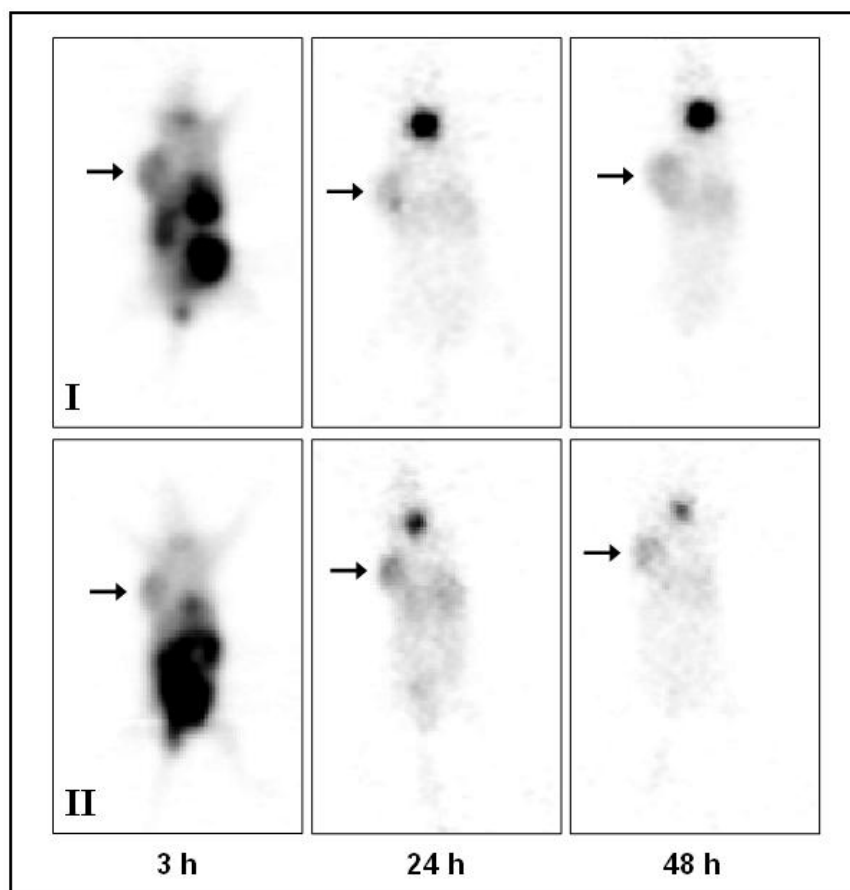
Figure 3: PET images of mice injected with [^{124}I]IAZA. Representative images 3 h, 24 h and 48 h following injection of [^{124}I]IAZA in two mice (I and II) breathing air; head at the top, tumor on left shoulder (arrow). Highest uptake in thyroid after 24h and 48 h.
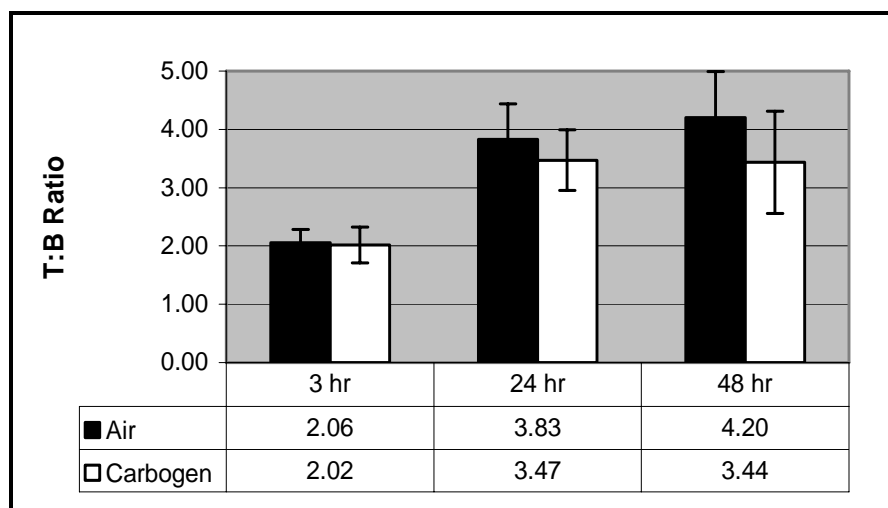
Figure 4: Tumor uptake of [124I]IAZA over 48 hours post injection. Tumor-to-background ratios of [124I]IAZA 3 h, 24 h and 48 h p.i. in Balb/c nude mice bearing A431 tumor, breathing either air or carbogen (Data are presented as mean with error bars indicating SD; for SD numbers see text; n = 4).

relevant to individualized and therefore optimized treatment planning (24-26) as well as an efficient therapy control (27). The aim of the current study was to investigate the potential of IAZA labeled with I-124 as a PET hypoxia tracer in comparison with its F-18 analog [18F]FAZA and the more established PET hypoxia tracer [18F]FMISO.

Optimum results in PET imaging depend predominantly on the pharmacokinetics of the radiotracer and the half-life of the radionuclide. Previous studies have shown that tumor-to-background ratios increase with uptake time in case of both [18F]FMISO and [18F]FAZA (12,13) and uptake times of approximately 3 h were found favorable in these small animal experiments due to the half-life of F-18. Using I-124 with its longer half-life gives the possibility of longer uptake times and late imaging. In the study presented here, 24 h and 48 h were chosen as late time points for imaging. At 3 h p.i. [18F]FAZA gave the highest T/B ratio, most likely due to slower clearance of [18F]FMISO from normal tissues. These comparative results are in very good agreement with previous studies (13). For [124I]IAZA clearance was much slower. One reason for this effect may be attributed to the different lipophilicities of the tracers. Partition coefficients (*P*) for the three compounds are 1.10

for FAZA, 2.60 for FMISO and 4.98 for IAZA (11). The most hydrophilic tracer, [18F]FAZA showed the best clearance. At 24 h and 48 h p.i. clearance was very good for [124I]IAZA, with the thyroid remaining as the only tissue with higher uptake than the tumor. However, T/B ratios for [124I]IAZA at 48 h were slightly lower than for [18F]FAZA after 3 h. The hypothesis that longer uptake times would result in significantly improved T/B ratios for [124I]IAZA could not be confirmed in this study. The major disadvantage of imaging at such late time points is the low absolute whole body activity after 48 h. From 24 h to 48 h there was almost no improvement in image quality. Therefore, it may be even advantageous to image after 12 h, with possibly still good clearance, some reduction in T/B ratio but higher count rates with a given administered activity. Blocking the thyroid by prior administration of iodide to the animals may be desirable.

Carbogen breathing resulted in reduced T/B ratios, particularly at the 3 h time point demonstrating again the oxygen dependence of uptake of the azomycin derivatives. This was more pronounced in the case of [18F]FAZA and less so for [124I]IAZA.
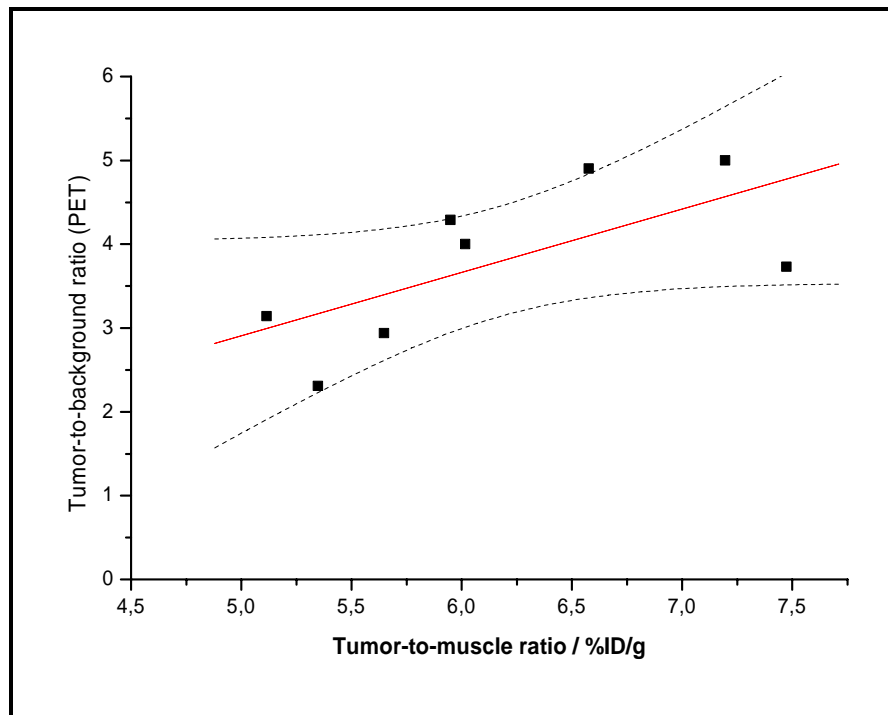
Figure 5: Regression analysis of data derived from ex vivo counting versus PET imaging for mice injected with [124I]IAZA. Correlation of T/M ratio (from biodistribution) and T/B ratio (from small animal PET) 48 h after injection of [124I]IAZA. Data are from 8 animals breathing air or carbogen (regression line $y = 0.76x - 0.87$; adjusted $r^2 = 0.46$; $P < 0.07$; dotted lines: 95 % confidence intervals).

PET results were in good agreement with the biodistribution data, both qualitatively and quantitatively as shown for [124I]IAZA (Figure 5) by comparing T/B ratios derived from PET with the T/M ratios derived from the tissue assays. Regression analysis resulted in a linear correlation for this tracer (regression line $y = 0.76x - 0.87$; adjusted $r^2 = 0.46$; $P < 0.07$; dotted lines: 95 % confidence intervals).

CONCLUSIONS

Although the number of animals involved in this study was limited, the results confirm the favorable properties of [18F]FAZA over [18F]FMISO for hypoxia imaging with PET due to its better clearance from background tissues after 3 h p.i. Oxygen dependent uptake was demonstrated for [18F]FAZA by having one group of mice breathing air, the other carbogen. To our knowledge, this is the first report of the use of [124I]IAZA in a small animal PET study. While 3 h [124I]IAZA PET images showed a high background, after 24 h and 48 h background was

very low (except for thyroid, for which iodide blocking would be advantageous). However, tumor activity was low as well, resulting in T/B ratios comparable to those of [18F]FMISO, but lower than for [18F]FAZA. Ex-vivo biodistribution data confirmed PET imaging findings.

From the data presented here [18F]FAZA appears to have superior properties for hypoxia imaging with PET compared to [18F]FMISO and [124I]IAZA. Nevertheless, further validations of [124I]IAZA are necessary (e.g. at time points between 3 and 24 h) to investigate its value for hypoxia PET imaging particularly at later time points.

ACKNOWLEDGEMENTS

at PMCI. The authors wish to acknowledge the expert technical assistance of Susan Jackson and Leigh Mathieson.

REFERENCES

[1] Teicher, B.A. Angiogenesis and cancer metastases: therapeutic approaches. Crit. Rev. Oncol. Hematol., 20: 9-39, 1995.

[2] Höckel, M., Schlenger, K., Aral, B., Mitze, M., Schaffer, U., Vaupel, P. Association between tumor hypoxia and malignant progression in advanced cancer of the uterine cervix. Cancer Res., 56: 4509-4515, 1996.

[3] Harrison, L.B., Chadha, M., Hill, R.J., Hu, K., Shasha, D. Impact of tumor hypoxia and anemia on radiation therapy outcomes. Oncologist, 7: 492-508, 2002.

[4] Krause, B.J., Beck, R., Souvatzoglou, M., Piert, M. PET and PET/CT studies of tumor tissue oxygenation. Q. J. Nucl. Med. Mol. Imaging, 50: 28-43, 2006.

[5] Chapman, J.D. Hypoxic sensitizers--implications for radiation therapy. N. Engl. J. Med., 301: 1429-1432, 1979.

[6] Chapman, J.D., Zanzonico, P. ,Ling, C.C. On measuring hypoxia in individual tumors with radiolabeled agents. J. Nucl. Med., 42: 1653-1655, 2001.

[7] Rasey, J., Koh, W., Evans, M., Peterson, L., Lewellen, T., Graham, M., Krohn, K. Quantifying regional hypoxia in human tumors with positron emission tomography of [18]Ffluoromisonidazole: a pretherapy study of 37 patients. Int. J. Radiat. Oncol. Biol. Phys., 24: 417-428, 1996.

[8] Rajendan, J.G., Wilson, D.C., Conrad, E.U., Peterson, L.M., Bruckner, J.D., Rasey, J.S., et al. [18]FFMISO and [18]FFDG PET imaging in soft tissue sarcomas: correlation of hypoxia, metabolism and VEGF expression. Eur. J. Nucl. Med. Mol. Imaging, 30: 695-704, 2003.

[9] Piert, M., Machulla, H.J., Becker, G., Stahlschmidt, A., Patt, M., Aldinger, P., Dissmann, P.D., Fischer, H., Bares, R., Becker, H.D., Lauchart, W. Introducing fluorine-18 fluoromisonidazole positron emission tomography for the localisation and quantification of pig liver hypoxia. Eur. J. Nucl. Med., 26: 95-109, 1999.

[10] Piert, M., Machulla, H.J., Becker, G., Aldinger, P., Winter, E., Bares, R. Dependency of the [18]Ffluoromisonidazole uptake on oxygen delivery and tissue oxygenation in the porcine liver. Nucl. Med. Biol., 27: 693-700, 2000.

[11] Kumar, P., Stypinski, D., Xia, H., McEwan, A.J.B., Machulla, H.J., Wiebe, L.I. Fluoro-azomycin arabinoside (FAZA): Synthesis, ^{2}H and ^{3}H-labelling and preliminary biological evaluation of a novel 2-nitroimidazole marker of tissue hypoxia. J. Labelled Compds. Radiopharm., 42: 3-16, 1999.

[12] Sorger, D., Patt, M., Kumar, P., Wiebe, L.I., Barthel, H., Seese, A., Dannenberg, C., Tannapfel, A., Kluge, R., Sabri, O. [^{18}F]Fluoroazomycin arabinofuranoside ([18]FAZA) and [^{18}F]Fluoro-misonidazole ([18]FMISO): A comparative study of their selective uptake in hypoxic cells and PET imaging in experimental rat tumors. Nucl. Med. Biol., 30: 317-326, 2003.

[13] Piert, M., Machulla, H.J., Picchio, M., Reischl, G., Ziegler, S., Kumar, P., Wester, H.J., Beck, R., McEwan, A.J.B., Wiebe, L. I., Schwaiger, M. Hypoxia-specific tumor imaging with 18F-fluoroazomycin arabinoside. J. Nucl. Med., 46: 106-113, 2005.

[14] Souvatzoglou, M., Roeper, B., Grosu, A., Machulla, H.J., Picchio, M., Beck, R., Wiebe, L.I., Molls, M., Schwaiger, M., Piert, M. Tumor hypoxia imaging with ^{18}F-FAZA in head & neck cancer. A pilot study. J. Nucl. Med., 46: 43P, 2005.

[15] Mannan, R.H., Somayaji, V.V., Lee, J., Mercer, J.R., Chapman, J.D., Wiebe, L.I. Radioiodinated 1-(5-iodo-5-deoxy-beta-D-arabinofuranosyl)-2-nitroimidazole (iodoazomycin arabinoside: IAZA): a novel marker of tissue hypoxia. J Nucl Med, 32:1764-1770, 1991.

[16] Kumar, P., McQuarrie, S.A., Zhou, A., McEwan, A.J. and Wiebe, L.I. [131]IIodoazomycin arabinoside for low-dose-rate isotope radiotherapy: radiolabeling, stability, long-term whole-body clearance and radiation dosimetry estimates in mice. Nucl. Med. Biol., 32:647-653, 2005.

[17] Urtasun, R.C., McEwan, A.J., Parliament, M.B., Mercer, J.R., Mannan, R.H., Wiebe, L.I., Morin, C.,Chapman, J.D. Measurement of hypoxia in human tumours by non-invasive SPECT imaging of iodoazomycin arabinoside. Br. J. Cancer, 74: S209, 1996.

[18] Zanzonico, P., O'Donoghue, J., Chapman, J.D., Schneider, R., Cai, S., Larson, S., Wen, B., Chen, Y., Finn, R., Ruan, S., Gerweck, L., Humm, J., Ling, C. Iodine-124-labeled iodoazomycin-galactoside imaging of tumor hypoxia in mice with serial microPET scanning. Eur. J. Nucl. Med. Mol. Imaging, 31: 117-128, 2004.

[19] Reischl, G., Ehrlichmann, W., Bieg, C., Solbach, C., Kumar, P., Wiebe, L.I., Machulla H.J. Preparation of the Hypoxia Imaging PET Tracer [18]FFAZA: Reaction Parameters and Automation. Appl. Radiat. Isot., 62: 897-901, 2005.

[20] Solomon, B., Binns, D., Roselt, P., Wiebe, L.I.,

McArthur, G.A., Cullinane, C., Hicks, R.J. Modulation of intratumoral hypoxia by the epidermal growth factor receptor inhibitor gefitinib detected using small animal PET imaging. Mol. Cancer Ther., 4: 1417-1422, 2005.

[21] Parliament, M.B., Chapman, J.D., Urtasun, R.C., McEwan, A.J., Goldberg, L., Mercer, J.R., Mannan, R.H., Wiebe, L.I.,Non invasive assessment of human tumour hypoxia with ^{123}I-iodoazomycin arabinoside: preliminary report of a clinical study. Br. J. Cancer, 65: 90-95, 1992.

[22] Johnson, C.A., Seidel, J., Carson, R.E., Gandler, W.R., Sofer, A., Green, M.V., Daube-Witherspoon, M.E. Evaluation of 3D reconstruction algorithms for a small animal PET camera. IEEE Trans. Nucl. Sci., 44, 1997.

[23] Lartizien, C., Kinahan, P.E., Swensson, R., Comtat, C., Lin, M., Villemagne, V., Trébossen, R. Evaluating image reconstruction methods for tumor detection in 3-dimensional whole-body PET oncology imaging. J. Nucl. Med., 44: 276-290, 2003.

[24] Brizel, D.M., Dodge, R.K., Clough, R.W., Dewhirst, M. W. Oxygenation of head and neck cancer: changes during radiotherapy and impact on treatment outcome. Radiother. Oncol., 53: 113-117, 1999.

[25] Eschmann, S.M., Paulsen, F., Reimold, M., Dittmann, H., Welz, S., Reischl, G., Machulla, H.J., Bares, R. Prognostic impact of hypoxia-imaging with ^{18}F-Misonidazole-PET in non-small cell lung cancer and head-and-neck cancer prior to radiotherapy. J. Nucl. Med., 46: 253-260, 2005.

[26] Rischin, D., Hicks, R.J., Fisher, R., Binns, D., Corry, J., Porceddu, S., Peters, L.J. Prognostic significance of ^{18}F-misonidazole positron emission tomography-detected tumor hypoxia in patients with advanced head and neck cancer randomly assigned to chemoradiation with or without tirapazamine: a substudy of Trans-Tasman Radiation Oncology Group study 98.02. J. Clin. Oncol., 24: 2098-2104, 2006.

[27] Dorow, D.S., Cullinane, C., Conus, N., Roselt, P., Binns, D., McCarthy, T.J., McArthur, G.A., Hicks, R.J. Multi-tracer small animal PET imaging of the tumour response to the novel pan-Erb-B inhibitor Cl-1033. Eur. J. Nucl. Med. Mol. Imaging, 33: 441-452, 2006.